J Mater Sci (2007) 42:6377–6381
DOI 10.1007/s10853-006-1187-0

Initial stages of the cubic-InN growth with the technique of the pre-deposition of indium

Z. X. Bi · R. Zhang · Z. L. Xie · X. Q. Xiu · Y. D. Ye · B. Liu · S. L. Gu · B. Shen · Y. Shi · Y. D. Zheng

Received: 24 April 2005 / Accepted: 27 October 2006 / Published online: 24 April 2007
© Springer Science+Business Media, LLC 2007

Abstract The initial stages of the cubic indium nitride film growth at 350 °C were studied using low-pressure metal-organic chemical vapor deposition. The technique of the pre-deposition of indium was applied, that is, a layer of indium was first deposited on sapphire surface before the growth of InN. X-ray diffraction and X-ray photoelectron spectroscopy show that the pre-deposition of indium is able to promote the growth of InN films, and meanwhile, suppress the indium aggregation in the as-grown films. Atomic force microscopy images of InN films indicate that the pre-deposition of indium not only enhances the density of nucleate sites, but also facilitates the coalescence among the InN islands. The free energy calculations reveal that the pre-deposited indium atoms preferentially react with NH and N radicals after NH_3 introduction, which leads to the formation of InN on the sapphire surface. The preferentially formed InN is then supposed to be responsible for the above phenomena.

Introduction

β-nitride semiconductors (AlN, GaN, InN and their alloys) have been paid much attention because of the potential applications in optoelectronic and microelectronic devices. Among the β-nitrides, InN has the smallest electron effective mass, the largest mobility, the highest peak and saturation electron drift velocities, and the smallest direct band gap [1, 2]. These distinguished properties make InN an interesting material for the applications in high-speed electronic devices and full-color displays [1–3]. However, until now, InN has not obtained enough study, because it is difficult to grow high-quality InN films. One obstacle for the growth of InN is the extremely high equilibrium vapor pressure of nitrogen. The low decomposition ratio of ammonia due to the low growth temperature of InN makes this problem more serious [4]. The other obstacle is the lack of lattice-matched substrate. As far as we know, sapphire is still the widely used substrate. However, the mismatch between sapphire and InN is 25% so that there exist high-density structural defects in InN films [1, 5, 6].

Recent studies on InN reveal that its band gap (E_g) is less than 1 eV, not the value of 1.9 eV reported in the earlier literatures [1, 7, 8]. The study of the band-gap bowing of $In_{1-x}Al_xN$ with respect to x also indicates that the E_g of InN should be less than 1.9 eV [7]. Davydov et al. indicated that the discrepancy with the earlier data on E_g could be explained by the improved quality of InN films [9]. Moreover, Inushima et al. and Miura et al. showed that InN films with E_g less than 1.5 eV presented anomalous electrical characteristics, that is, a sharp decrease of resistivity and a sharp increase of mobility were observed at temperatures less than 4.2 K [7, 10]. So in order to investigate the fundamental properties of InN, it is necessary to grow high quality InN films.

Compared with InN films grown by molecular beam epitaxy (MBE), InN films grown by metal-organic chemical vapor deposition (MOCVD) have inferior electrical properties due to the deficient decomposition of ammonia. However, Bhuiyan et al. indicated that if the decomposition of ammonia was enhanced, the electrical properties of

Z. X. Bi · R. Zhang (✉) · Z. L. Xie · X. Q. Xiu · Y. D. Ye · B. Liu · S. L. Gu · B. Shen · Y. Shi · Y. D. Zheng
Key Laboratory of advanced Photonic and Electronic Materials, Department of Physics, Nanjing University, Nanjing 210093, China
e-mail: rzhang@nju.edu.cn

InN grown by MOCVD could be significantly improved [11]. With the enhanced decomposition of ammonia, Yamamoto et al. obtained MOCVD-grown InN films with the Hall mobility of 700–800 cm^2/Vs and the background electron concentration of 10^{18} cm^{-3} [12]. As the GaN growth on sapphire substrates, InN films are also deposited with the buffer layer technique in terms of either MBE [3, 6, 13, 14] or MOCVD [15]. With the low temperature InN/GaN buffer layers, the Hall mobility and the background electron concentration of MBE-grown InN film have reached 1,420 cm^2/Vs and 1.4×10^{18} cm^{-3}, respectively [13]. Therefore, in order to further enhance the quality of InN films, the understanding of the buffer layer growth at the low temperature is necessary.

In this work, we deposited InN films on sapphire substrates at the temperature of 350 °C which is commonly used for the growth of the InN buffer layers. The technique of the pre-deposition of indium was applied. We found that suitable pre-deposition of indium could not only promote the nucleation and the growth of InN, but also facilitate the coalescence among InN islands.

Experimental details

InN films in this work were deposited on (0001)-oriented sapphire substrates using home-made low-pressure MOCVD. The details of our MOCVD can be found in Ref. [16]. Ammonia (NH_3) and trimethylindium (TMIn) were used as N and In precursors, respectively. TMIn was kept at 40 °C, and was carried into the chamber by hydrogen gas. Sapphire substrates were firstly cleaned with organic solvents in an ultrasonic bath, and then etched in H_2SO_4:H_3PO_4 = 3:1 solution at 170 °C for 5 min. After loaded into the chamber, sapphire substrates were heated at 900 °C for 10 min in hydrogen ambience, followed by the nitridation in NH_3 ambience for 30 min. Then, the temperature was decreased to 350 °C in order to grow InN. Before the growth of InN, a layer of indium was firstly deposited on sapphire substrate with TMIn as the precursor. Subsequently, NH_3 was transported into the chamber, and the InN growth commenced. Changing the time for the indium pre-deposition, a series of InN films was prepared. The flow rates of TMIn and NH_3 were 4.3 μmol/min and 0.08 mol/min, respectively. The pressure in the chamber was set to 53 mbar, and the growth time was 90 min.

$\theta/2\theta$ X-ray diffraction (XRD) and X-ray photoelectron spectroscopy (XPS) of the as-grown InN films were measured, which were used to analyze the InN growth and the indium aggregation in the grown layer. In addition, the surface morphology of InN was observed by Atomic force microscopy (AFM).

Results and discussion

Figure 1 shows the $\theta/2\theta$ XRD spectra of the InN samples grown with a layer of indium pre-deposited for different time. Spectra (a)–(e) correspond to the indium pre-deposition time of 0, 5 min, 10 min, 15 min, and 20 min, respectively. In each spectrum, a diffraction peak at $2\theta = 31.1°$ can be found. This position is consistent with that of cubic-InN(111) diffraction peak, which indicates that the structure of the as-grown InN is cubic. As the growth temperature is 375 °C, this diffraction peak positively shifts to $2\theta = 31.3°$ (not shown here), which corresponds to hexagonal InN(0002) plane. The other peaks at $2\theta = 32.9°$ in Fig. 1 originate from the diffraction of In(101) plane. It is obvious that the time for the indium pre-deposition has an important influence on the aggregation of indium in the grown layers. With increasing the indium pre-deposition time, the diffraction peaks of cubic-InN(111) are intensified, but the intensity of In(101) peaks

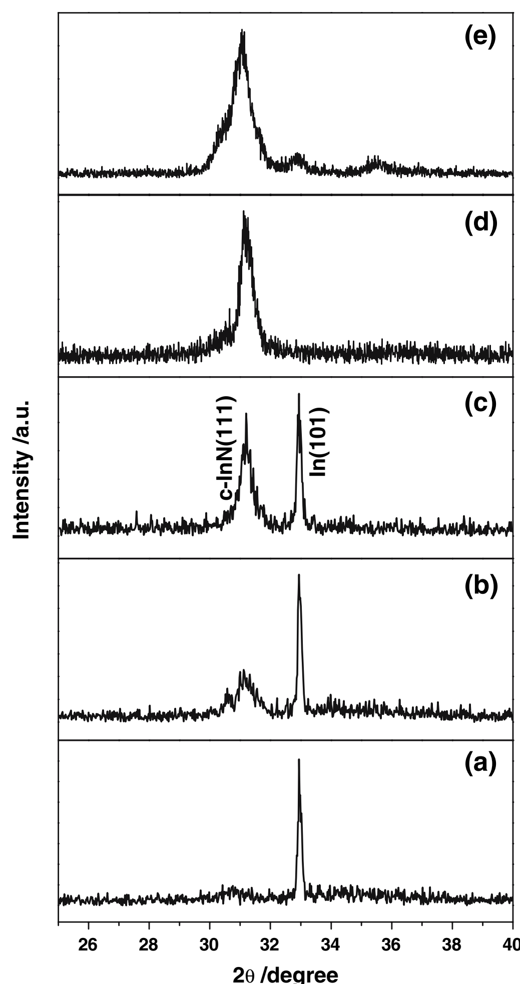

Fig. 1 $\theta/2\theta$ XRD spectra of the cubic-InN samples grown on (0001)-oriented sapphire substrates with a layer of indium pre-deposited for (**a**) 0, (**b**) 5 min, (**c**) 10 min, (**d**) 15 min, and (**e**) 20 min

is lowered. As the time for the indium pre-deposition is 15 min, the peak from In(101) disappears completely, and only one peak from InN(111) can be observed. However, as the indium pre-deposition time is 20 min, the diffraction peak from In(101) appears again. This indicates that 15 min is the optimum duration for the indium pre-deposition. Figure 2 shows the XPS $In_{3d5/2}$ and $In_{3d3/2}$ spectra of the InN samples grown with a layer of indium pre-deposited for 0 and 15 min. The peak positions are calibrated using the C 1s peak as a reference at 284.6 eV. The $In_{3d5/2}$ peak of the InN sample grown without the indium pre-deposition is at 443.7 eV [Fig. 2a], which is very close to the value of 443.6 eV of $In_{3d5/2}$ in In–In bond. This means that the indium aggregation is serious as there is no pre-deposition of indium. This result is consistent with the XRD spectrum shown in Fig. 1a. In the XPS spectrum of the InN grown with a layer of indium pre-deposited for 15 min, the $In_{3d5/2}$ peak positively shifts to 444.4 eV [Fig. 2b]. Parala et al. reported the binding energy of 444.3 eV of $In_{3d5/2}$ in In–N bond [17]. Thus, our result is identical with this value, which means that there is no indium aggregation in the InN as the indium pre-deposition time is 15 min. This XPS result is also consistent with the XRD spectrum shown in Fig. 1d.

Figure 3 shows the AFM images of the five InN samples shown in Fig. 1. Without the pre-deposition of indium, there are only a few islands on the surface [Fig. 3a]. However, as the indium is pre-deposited for 5–20 min [Fig. 3b–e], the density of islands increased intensively, which indicates that the pre-deposition of indium can promote the nucleation of InN. Meanwhile, the lateral size of islands increases gradually, that is, the horizontal growth rate is increased. In terms of the pre-deposition time of 20 min, the islands begin to coalesce. In addition, with the increment of the indium pre-deposition time from 0 to 15 min, the roughness mean square (RMS) of InN films increases from 0.578 to 4.541 nm [Fig. 3a–d]. As the indium pre-deposition time is 20 min, RMS is 3.789 nm [Fig. 3e], which is lower than 4.541 nm shown in Fig. 3d. This also indicates that the horizontal growth rate increases with the indium pre-deposition time, and the increment of the lateral growth suppresses the vertical growth of the islands.

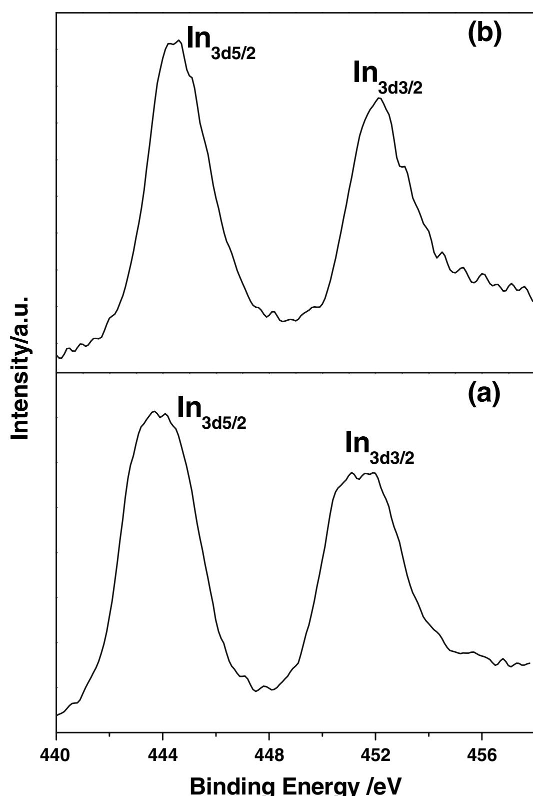

Fig. 2 XPS $In_{3d5/2}$ and $In_{3d3/2}$ spectra of the InN samples grown with a layer of indium pre-deposited for (**a**) 0, and (**b**) 15 min

From the description above, it is concluded that the pre-deposition of indium is able to promote the growth of InN and facilitate the coalescence among the InN islands. Thermodynamically, NH_3 can be decomposed into N_2 and H_2 at temperatures higher than 300 °C [18]. Therefore, after the introduction of NH_3 into the chamber, the pre-deposited indium can possibly react with NH_3, NH_2, NH and N radicals, besides the reaction with the indium gas decomposed from TMIn. In this work, the pre-deposited indium exists on the surface of sapphire in the state of liquid, because the melting point of indium is 156 °C. The chemical reactions and the corresponding changes of the free energy ($\Delta G°$) at 350 °C are listed in Table 1. In the case of the reactions of the pre-deposited indium with indium gas, NH_2, NH and N radicals, the values of $\Delta G°$ are negative, which means that these reactions may happen on the surface. In terms of the reactions of the pre-deposited indium with NH and N radicals, the changes of the free energy are larger than that of the reaction between the pre-deposited indium and indium gas. This indicates that the pre-deposited indium preferentially reacts with NH and N radicals, which leads to the formation of InN on sapphire surface. The preferentially formed InN can act as the nucleation sites for the subsequent InN growth. This is the reason why the pre-deposition of indium can increase the density of the InN islands shown in Fig. 3b–e. The supply of the nucleation sites for the InN growth enhances the sticking ratio of nitrogen atoms into the growth front, which suppresses the aggregation of indium in the InN films. Figure 1d indicates that 15 min is suitable for the indium pre-deposition in order to provide enough nucleation sites for the InN growth. As the indium is pre-deposited for longer than 15 min, the indium aggregation appears again [Fig. 1e]. The reason for this is that the pre-deposited indium is too much, and there is no enough NH and N radicals to react with the pre-deposited indium due to the low dissociation ratio of NH_3.

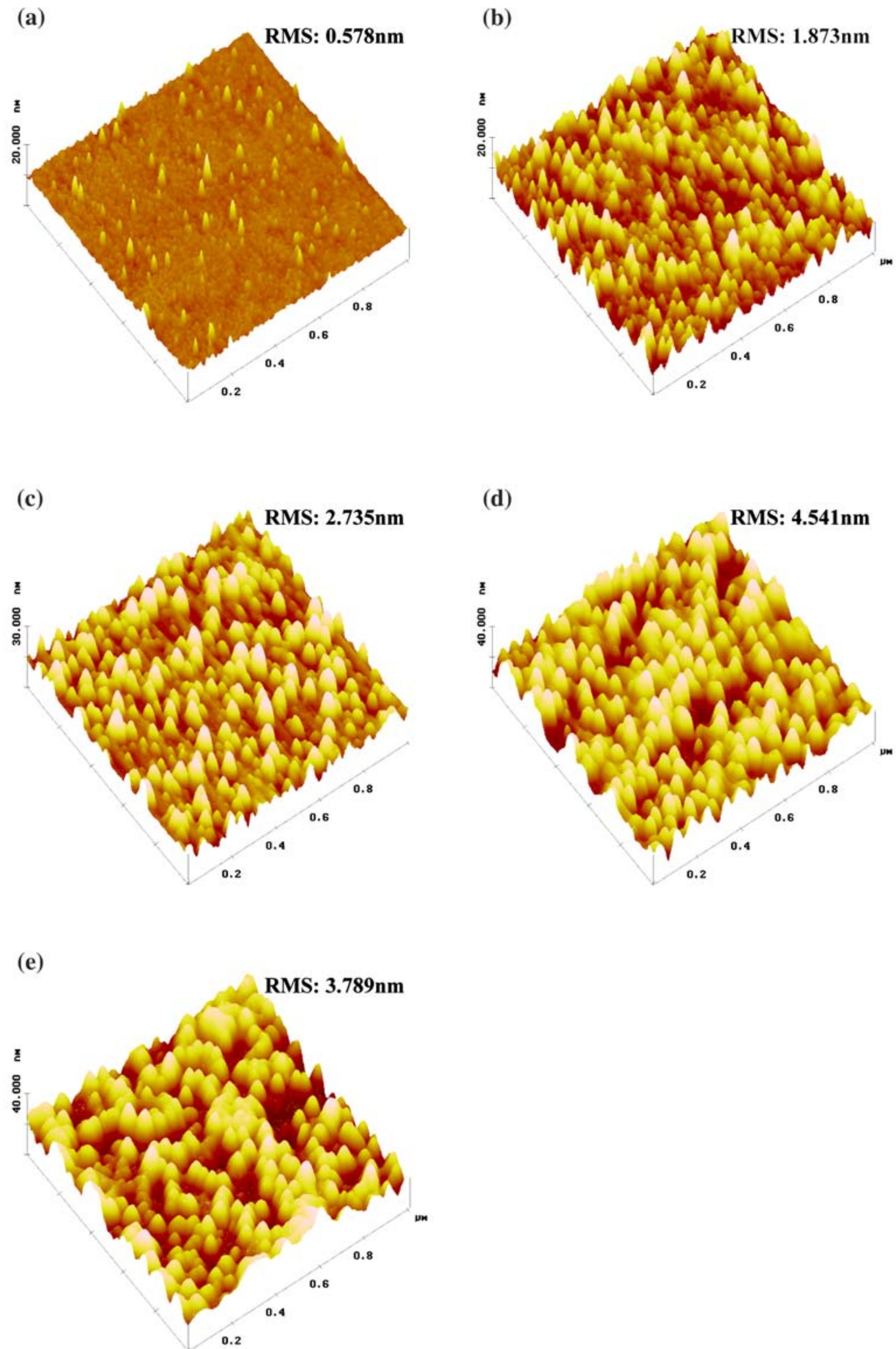

Fig. 3 AFM images of the InN samples shown in Fig. 1 with a layer of indium pre-deposited for (**a**) 0, (**b**) 5 min, (**c**) 10 min, (**d**) 15 min, and (**e**) 20 min

Conclusions

We have grown (111)-oriented cubic InN films on (0001)-oriented sapphire substrates using low-pressure MOCVD. XRD and XPS measurements indicate that the technique of the indium pre-deposition plays a key role on the InN growth at 350 °C. With the suitable pre-deposition of indium, cubic-InN without the indium aggregation can be obtained. In our work, 15 min is the optimum duration for the pre-deposition of indium. AFM images show that the pre-deposition of indium is able to increase the density of the InN nucleation sites, and be favor of the coalescence among the InN islands. The reason for the above phenomena is that the reactions of the pre-deposited indium

Table 1 The chemical reactions of the pre-deposited indium with the indium gas, NH_3, NH_2, NH and N radicals, and the corresponding changes of the free energy ($\Delta G°$) at the temperature of 350 °C

Chemical reaction	$\Delta G°$ at 350 °C (kJ/mol)
In(l) + In(g) = 2In(l)	–172.748
In(l) + NH_3(g) = InN(s) + 3/2H_2(g)	34.541
In(l) + NH_2(g) = InN(s) + H_2(g)	–158.412
In(l) + NH(g) = InN(s) + 1/2H_2(g)	–311.083
In(l) + N(g) = InN(s)	–383.096

atoms with NH and N radicals can provide the nucleation sites for the InN growth, promote the sticking of the nitrogen atoms, and then suppress the indium aggregation in the as-grown InN films.

Acknowledgements This work is supported by Special Funds for Major State Basic Research Project G2000068305, Hi-tech Research Project (2003AA311060, 2001AA311110), Distinguished Young Scientist Grant (60025411) and National Nature Science Foundation of China (60290083, 60136020).

References

1. Nanishi Y, Saito Y, Yamaguchi T (2003) Jpn J Appl Phys 42:2549
2. Yang FH, Hwang JS, Yang YJ, Chen KH, Wang JH (2002) Jpn J Appl Phys 41:L1321
3. Higashiwaki M, Matsui T (2002) Jpn J Appl Phys 41:L540
4. Matsuoka T, Nakao M, Okamoto H, Harima H, Kurimoto E (2003) Jpn J Appl Phys 42:2288
5. Tsuchiya T, Ohnishi M, Wakahara A, Yoshida A (2000) J Cryst Growth 220:191
6. Saito Y, Yamaguchi T, Kanazawa H, Kano K, Araki T, Nanishi Y, Teraguchi N, Suzuki A (2002) J Cryst Growth 237–239:1017
7. Inushima T, Mamutin VV, Vekshin VA, Ivanov SV. Sakon T, Motokawa M, Ohoya S (2001) J Cryst Growth 227–228:481
8. Saito Y, Harima H, Kurimoto E, Yamaguchi T, Teraguchi N, Suzuki A, Araki T, Nanishi Y (2002) Phys Stat Sol (b) 234(3):796
9. Davydov VY, Klochikhin AA, Emtsev VV, Ivanov SV, Vekshin VV, Bechstedt F, Furthmuller J, Harima H, Mudryi AV, Hashimoto A, Yamamoto A, Aderhold J, Graul J, Haller EE (2002) Phys Stat Sol (b) 230(2):R4
10. Miura N, Ishii H, Yamada A, Konagai M, Yamauchi Y, Yamamoto A (1997) Jpn J Appl Phys 36:L256
11. Bhuiyan AG, Tanaka T, Yamamoto A, Hashimoto A (2002) Phys Stat Sol (a) 194(2):502
12. Yamamoto A, Tanaka T, Koide K, Hashimoto A (2002) Phys Stat Sol (b) 194(2):510
13. Higashiwaki M, Matsui T (2003) J Cryst Growth 252:128
14. Saito Y, Teraguchi N, Suzuki A, Araki T, Nanishi Y (2001) Jpn J Appl Phys 40:L91
15. Bhuiyan AG, Yamamoto A, Hashimoto A, Ito Y (2002) J Cryst Growth 236:59
16. Shen B, Zhou YG, Chen ZZ, Chen P, Zhang R, Shi Y, Zheng YD, Tong W, Park W (1999) Appl Phys A 68:593
17. Parala H, Devi A, Hipler F, Maile E, Birkner A, Becker HW, Fischer RA (2001) J Cryst Growth 231:68
18. Koukitu A, Takahashi N, Taki T, Seki H (1996) Jpn J Appl Phys 35:L673